PAN ARCHIVES OF ACOUSTICS
Vol. **43**, No. 3, pp. 413–423 (2018)

DOI: 10.24425/123913

The Radiation Efficiency Measurements of Real System of a Thin Circular Plate Embedded Into a Thick Square Baffle

Krzysztof SZEMELA, Wojciech P. RDZANEK, Wojciech ŻYŁKA

Department of Mechatronics and Control Science
Faculty of Mathematics and Natural Sciences
University of Rzeszów
Pigonia 1, 35-310 Rzeszów, Poland; e-mail: alpha@ur.edu.pl

(*received March 5, 2018; accepted May 21, 2018*)

Most of sound sources are complex vibroacoustic objects consist of numerous elements. Some coupled vibrating plates of different shapes and sizes can be easily found in urban environments. The main aim of this study is to determine the sound radiation of coupled plates system of practical importance. The investigated vibroacoustic system consist of a thin circular plate coupled with a thick flat baffle with a circular hole. The circular plate has been mounted to the baffle's hole using screws and two steel rings. The measurement setup was located inside a semi-anechoic chamber to assure the free field conditions. It was necessary to take into account the whole system surface to obtain the radiation efficiency based on the Hashimoto's method. Such an approach can be troublesome and time-consuming. Therefore, the criterion has been proposed which allows the vibration velocity measurements and calculations to be performed only for the thin plate's area. An alternative approach has been proposed based on the classical Rayleigh integral formula. Its advantage is a simpler implementation in a computer code. The obtained results have been compared with the theoretical results obtained for the elastically supported circular plate. A good agreement has been obtained at low frequencies.

Keywords: radiation efficiency; measurements; Hashimoto's method; coupled plates.

1. Introduction

In practice, many real sound sources are complex vibroacoustic system of coupled vibrating structures. In many cases, the vibroacoustic objects consist of plates with different shapes, sizes as well as boundary configurations. The plates are commonly used in different branches of industry. They are elements of covers, transducers, microphones, windows, etc. Vibroacoustic properties of such elements are important. Therefore, radiation efficiency, acoustic insulation, acoustic impedance as well as vibration responses and acoustic fields associated are under constant focus of many researchers. Theoretical studies, though numerous, are often complex and therefore limited to the simplest cases (Kwak, Kim, 1991; Amabili *et al.*, 1996; Lee, Singh, 1994; Rdzanek *et al.*, 2003; 2007; 2016; Wiciak, 2007; Oberst *et al.*, 2013; Jeong, 2003; Jeong, Kim, 2005; Gazizullin, Paimushin, 2016; Hasheminejad, Afsharmanesh, 2014; Christiansen *et al.*, 2014; Shahraeeni *et al.*, 2015; Squicciarini *et al.*, 2015; Liu *et al.*, 2017). Consequently, experimental methods of analysis are widely accepted due to obvious shortcomings and limitations of the theoretical methods. The results of both theoretical and experimental investigations are often used in different practical applications such as active control of noise and vibrations (Leniowska, 2006; Branski, Szela, 2011; Mazur, Pawełczyk, 2011; Kozupa, Wiciak, 2011; Yuan *et al.*, 2011; 2012; Leniowska, Mazan, 2015; Hasheminejad, Keshavarzpour, 2016; Mazur, Pawełczyk, 2016; Beigelbeck *et al.*, 2013; Sun *et al.*, 2015), sensors and speakers (Vishwakarma *et al.*, 2014; Chiang, Huang, 2015; 2018), and some modal tests (Matthews *et al.*, 2014; Robin *et al.*, 2016; Zhao *et al.*, 2016; Kamper, Bekker, 2017). The discretisation technique has been used to investigate the sound radiation inside a layer bounded by two walls (Díaz-Cereceda *et al.*, 2012). The method of measuring the radiation efficiency of vibrating flat structures by its discretization has been widely accepted. The method has been originally proposed by Hashimoto (2001). Further, it has been developed significantly by Arenas

and Crocker (2002), Arenas (2008; 2009a; 2009b; 2010). The Hashimoto's method has been further developed theoretically by Luo *et al.* (2015). The method was also used for some other theoretical and experimental analyses of the radiation efficiency of vibrating surface sources by Hu and Shang (2012), Xiaoqing *et al.* (2014), Kolber *et al.* (2014), Wang and Xiang (2017), Jiang *et al.* (2017), Langfeldt *et al.* (2018), Jung *et al.* (2017).

A thin plate mounted to a thick flat screen constitutes a coupled system of practical importance. Such a vibroacoustic system can be easily found in architecture as well as in industry. It can be considered as a cover or window represented by a thin plate embedded in a building wall which is thick flat baffle. This study is focused on determining the radiation efficiency of a system of the two coupled plates. The investigated object is the thin steel circular plate with a point excitation embedded in a flat thick rectangular baffle. In order to make the analyzed problem more practical, the circular plate has been mounted to the flat screen using one of the most common mounting method, i.e., the mounting by means of screws. The radiation efficiency of the considered system can been obtained based on the Hashimoto's method. However, this approach is time-consuming, troublesome or even impossible when a sound source surface has to be divided into a large number of discrete elements. Hence, it is necessary to propose the procedure which allows an approximate value of the radiation efficiency to be found in a convenient way. Although the baffle and the circular plate constitute a system of two coupled plates, the baffle is much thicker than the circular plate. Therefore it is supposed that for some frequencies the effect of vibrational interactions between the two plates can be neglected which makes the baffle's vibration velocity much smaller than the vibration velocity of the circular plate. The criterion for such a negligence will be described later on in more detailed way. Generally it is accepted that if the means square vibration velocity on the baffle is much smaller than on the circular plate, the negligence can be applied. This means that in some cases, the baffle's contribution to the sound radiation can be negligible small and the radiation efficiency of the coupled plates can be approximately determined as the radiation efficiency of the thin plate only. This allows the vibration velocity measurements as well as calculations to be performed only for the thin plate area and consequently reduces measurement procedure complexity. Therefore, another aim of this study is to define the criterion to indicate the conditions for which such simplification is possible.

2. Normalized sound power

The normalized sound power, one of the fundamental quantities describing the properties of an acoustic source, can be calculated from the following formula (cf. Skudrzyk (1971) Sec. 28.3 Eqs. (18)–(24); and Arenas (2009a) Eq. (15))

$$\Pi/\Pi^{(\infty)} = \sigma - \mathrm{i}\kappa, \tag{1}$$

where Π is the time average complex sound power, $\Pi^{(\infty)} = \lim_{k\to\infty}\Pi = \rho_0 c S\langle|v|^2\rangle_S$ is the reference sound power radiated for the infinite value of the acoustic wavenumber $k = 2\pi f/c$, f is the vibration frequency, S is the sound source area, c and ρ_0 denote the speed of sound and the density of air, respectively,

$$\langle|v|^2\rangle_{S_a} = \frac{1}{2S_a}\int\limits_{S_a}|v|^2\,\mathrm{d}S_a, \tag{2}$$

is the time-averaged mean square vibration velocity calculated for an arbitrary surface S_a enclosing the sound source (cf. Arenas (2009a) Eq. (16)), σ is the radiation efficiency and $\kappa = 2\pi f\mu$ is the added mass coefficient, μ is the total effective mass of the plate (after Skudrzyk (1971) Sec. 28.3 the text after Eq. (19)), and i is the imaginary unit. To determine the quantities σ and κ, it is necessary to find the sound power. The experimental investigations of the sound power based on the measurements of the sound intensity are troublesome and time-consuming. However, this quantity can be approximately determined in more convenient way by measuring only the vibration velocity at some discrete source points. Based on the impedance approach, the sound power can be expressed as (cf. Skudrzyk (1971) Sec. 28.3 Eq. (18))

$$\Pi = \frac{1}{2}\int\limits_{S} pv^*\,\mathrm{d}S, \tag{3}$$

where p is the acoustic pressure, v is the normal component of the vibration velocity of source points and the symbol * denotes the conjugate of any complex quantity.

The sound power can be calculated with the use of the two different methods. To use these methods, it is necessary to discretize the source surface, i.e., to divide it into virtual elements whose dimensions are small compared with the acoustic wave length λ. The vibration velocity is assumed to be uniformly distributed on the surface of each particular element. It is also convenient to divide a source surface into elements of the same areas ΔS which simplifies the obtained formulas. In the case of a circular source, such a discretization has been proposed by Arenas (2009a) (cf. his Sec. 2.3 and Fig. 1). It has been assumed that the locations of the central points of the elements are given by the set of vectors $\mathbf{r}_u$ for $u = 1, 2, \ldots, W$, where W is the number of elements. The time-average mean square vibration velocity for an arbitrary discretized surface S_a, in the case when all the virtual elements have the same

area ΔS, can be calculated as (cf. Arenas (2009a) Eq. (17))

$$\langle |v|^2 \rangle_{S_a} = \frac{\Delta S}{2S_a} \sum_u |v_u|^2, \tag{4}$$

where $v_u = v(\mathbf{r}_u)$ is the vibration velocity of the u-th element and the summation is performed over all the elements located on the surface S_a. After calculating the sound power Π, the radiation efficiency σ as well as the added mass coefficient κ can be obtained with by using Eqs. (1) and (4).

3. The Hashimoto's method

The sound power can be determined using the Hashimoto's method. This method is based on the assumption that the u-th virtual element can be considered as the piston of the vibration velocity v_u and the area ΔS. Then, using Eq. (3) results in (Hashimoto (2001) Eq. (3))

$$\Pi \simeq \frac{1}{2} Z^{(\text{self})} \sum_{u=1}^{W} |v_u|^2 + \sum_{u=2}^{W} \sum_{q=1}^{u-1} Z_{u,q}^{(\text{mut.})} \text{Re}(v_u v_q^*), \tag{5}$$

where $\text{Re}(\cdot)$ gives the real part of a complex quantity,

$$Z^{(\text{self})} = \rho_0 c \, \Delta S \left[1 - \frac{J_1(2ka_0)}{ka_0} - \text{i} \, \frac{\mathbf{H}_1(2ka_0)}{ka_0} \right], \tag{6}$$

is the self impedance (Hashimoto (2001) Eq. (1); cf. also Pritchard (1960) Eqs. (9) and (10)), $J_1(\cdot)$ is the Bessel function of first order, $\mathbf{H}_1(\cdot)$ is the Struve function of first order, $a_0 = \sqrt{\Delta S/\pi}$ is the piston radius, and

$$Z_{u,q}^{(\text{mut.})} = -2\text{i} \, \rho_0 c \, \Delta S J_1^2(ka_0) \, \frac{\text{e}^{\text{i}k|\mathbf{r}_u - \mathbf{r}_q|}}{k|\mathbf{r}_u - \mathbf{r}_q|}, \tag{7}$$

is the mutual impedance (Hashimoto (2001) Eq. (2); cf. also Pritchard (1960) Eq. (12)). The number of terms in Eq. (5) has been reduced taking into account that $Z_{u,q}^{(\text{mut.})} = Z_{q,u}^{(\text{mut.})}$ and $v_u v_q^* + v_q v_u^* = 2\text{Re}(v_u v_q^*)$ which significantly improves the sound power calculations.

4. The Rayleigh's method

The sound power from Eq. (3) can be formulated for the discretized source surface as

$$\Pi \simeq \frac{\Delta S}{2} \sum_{u=1}^{W} p_u v_u^*, \tag{8}$$

where $p_u = p(\mathbf{r}_u)$ is the sound pressure at the central point of the u-th element, and the integration of continuous quantity pv^* has been replaced by the summation of the discrete elements on a sound source surface leading to approximate results. The quantity p_u can be found using the Rayleigh's first integral (cf. Rayleigh (1896) Sec. 278)

$$p(\mathbf{r}) = -\text{i}f\rho_0 \int_S v(\mathbf{r}_S) \frac{\text{e}^{\text{i}k|\mathbf{r}-\mathbf{r}_S|}}{|\mathbf{r}-\mathbf{r}_S|} \, \text{d}S, \tag{9}$$

where $\mathbf{r}$ is the vector indicating field point, $\mathbf{r}_S$ is the source point vector. The above formula has been presented in the discrete form by using the auxiliary discretization. The area of each element of the auxiliary discretization is equal to ΔS and the locations of the elements' central points are given by the set of vectors $\mathbf{r}'_q$ for $q = 1, \ldots, W$. Next, the formula from Eq. (9) can be expressed as

$$p(\mathbf{r}) \simeq -\text{i}f\rho_0 \Delta S \sum_{q=1}^{W} v'_q \frac{\text{e}^{\text{i}k|\mathbf{r}-\mathbf{r}'_q|}}{|\mathbf{r}-\mathbf{r}'_q|}, \tag{10}$$

where $v'_q = v(\mathbf{r}'_q)$. Taking into account the singularity in Eq. (10), it is clear that the sound pressure p_u can be calculated only for the auxiliary discretization performed so that $\mathbf{r}_u \neq \mathbf{r}'_q$ for $u, q = 1, \ldots, W$. Finally, inserting Eq. (10) into Eq. (8) leads to

$$\Pi \simeq -\frac{1}{2} \, \text{i}f\rho_0 \Delta S^2 \sum_{u=1}^{W} \sum_{q=1}^{W} v'_q \, \frac{\text{e}^{\text{i}k|\mathbf{r}_u - \mathbf{r}'_q|}}{|\mathbf{r}_u - \mathbf{r}'_q|} \, v_u^*. \tag{11}$$

The above formula is equivalent for the formula from Eq. (5). In the further analysis, the results given by both formulas as well as their computational efficiencies have been discussed.

5. Measurement setup and instruments

The investigated object was a steel circular plate with the radius $a = 0.15$ m and the thickness $h = 1$ mm. It was mounted with the use of eight screws and two steel rings to a flat chipboard of the thickness 28 mm and with the width and the length equal to 1.7 m (see Fig. 1). The flat chipboard was considered as a baffle. It was situated on four columns filled with

Fig. 1. The investigated circular plate, mounting screws and steel ring.

sand which ensured a vibroacoustic insulation from vibrations of a building floor (see Fig. 2). The distance between the baffle and the chamber floor was equal to 72 cm. To reduce an influence of reflected waves as well as some other acoustics disturbances, the measurement setup has been placed inside the semi-anechoic chamber. The chamber's walls and ceiling are covered with wedges which absorb acoustic waves for frequencies $f > 200$ Hz. The chamber floor is a reflected surface. Therefore, some acoustic waves reflected from the floor can disturb acoustic measurements. This effect is particularly strong when the amplitude of acoustic pressure generated by some acoustic waves reflected from the floor has a maximum (see Appendix A). The plate vibrations were generated by a point excitation realized with the help of the shaker The Modal Shop 2075E. The excited point was asymmetrically located in the distance $0.75a$ from the plate center. This allowed some asymmetric modes to be strongly excited. The time dependence of the plate excitation was assumed in the form of the white noise which caused that the acoustic behavior of the considered system can be investigated for a whole analyzed frequency range. Moreover, the amplitude of excitation force was chosen so that the plate deflections can be small enough to describe its vibrations by the plate linear model. As a result of measurements, the vibration velocity of the plate as well as the baffle was determined using the Polytec PDV-100 vibrometer. Additionally, the value of excitation force F was measured by means of the PCB Piezotronics 208C03 force sensor. The measurements and data aggregation were performed with the use of the LMS Scadas Mobile data acquisition device and the LMS Test.Xpress software.

Fig. 2. The measurement setup placed inside the semi-anechoic chamber.

6. Vibration velocity measurements

In order to determine the measuring points' locations, the polar coordinate system with the origin placed at the thin plate central point and the radial axis including the plate's excited point has been introduced. In this coordinate system, the position vector has been defined as $\mathbf{r}_0 = (r_0, \varphi_0)$, where r_0 and φ_0 are the radial coordinate and the angular coordinate, respectively. Taking into account the construction of measurement setup, it can be expected that the thin plate's vibrations can generate the vibrations of the baffle. Hence, the considered sound source are the two coupled plates. The vibration velocity measurements were performed on the surface S_1 containing the points for which $0 < r_0 \leq a_1 = 3a = 0.45$ m. The measuring points' locations are given by the following set of vectors $\mathbf{r}_j^{(m)} = (r_j^{(m)}, \varphi_j^{(m)})$ where

$$\begin{aligned} r_j^{(m)} &= 25\lfloor (j+13)/15 \rfloor \text{ [mm]}, \\ \varphi_j^{(m)} &= \frac{2\pi}{15} \operatorname{mod}(j-2, 15)\gamma_j, \end{aligned} \tag{12}$$

$j = 1, \ldots, 271$, $\lfloor w \rfloor$ gives the greatest integer less than or equal to w, $\operatorname{mod}(a, b)$ is the reminder after division of a by b, $\gamma_1 = 0$ and $\gamma_j = 1$ for $j > 1$. The vibration velocity has been measured for some selected thin plate's points to provide an accurate information about a plate's vibrational behavior. The measurements performed at some baffle's points allows its contribution to the sound radiation of the considered system to be estimated. Because of a small value of the applied exciting force F [N], it has be assumed that the vibration velocity is proportional to the value of F and the following relation is satisfied

$$v(\mathbf{r}_0) = \beta(\mathbf{r}_0)F, \tag{13}$$

where $\beta(\mathbf{r}_0)$ [m/(s·N)] is the proportionality coefficient. The main aim of measurements was to determine the function $\beta(\mathbf{r}_0)$. For this purpose, the exciting force was recorded as a function of time for each velocity measurement. The duration of measurement in the case of each point was equal to 30 s and the sampling frequency 12.8 kHz. Based on the measurement data and making use of DFT (Discrete Fourier Transform), in the case of each measuring point j, the vibration velocity $v_j^{(m)}$ as well as the exciting force $F_j^{(m)}$ have been obtained for the discrete values of frequency $f = f_n$ where $f_n = n/30$ Hz for $n = 0, 1, \ldots$ Then, making use of Eq. (13) the values of the proportionality coefficient have been obtained at the measuring points as $\beta(\mathbf{r}_j^{(m)}) = v_j^{(m)}/F_j^{(m)}$. Finally, using an interpolation, the continuous functions $\beta(\mathbf{r}_0)$ defined on the whole investigated surface S_1 have been determined for the discrete frequencies f_n. These interpolating functions have been used in further numerical calculations.

7. Surface discretization

The considered circular surface S_1 has been discretized according to the method proposed by Arenas (2009a) (cf. his Sec. 2.3 and Fig. 1). Firstly, the

surface has been divided into rings of the same width $\Delta r = a_1/N$, where N is the number of rings. Then, in order to obtain the elements of the same area $\Delta S = \pi(\Delta r)^2/4$, the discretization has been perform assuming that the ring of number j, where $j = 1, \ldots, N$ contains $4(2j-1)$ elements. The number of all the elements is equal to $W_1 = 4N^2$ whereas the number of elements located on the thin plate's surface can be expressed as $W = a^2 W_1/a_1^2$. The vectors defining the locations of elements' central points can be expressed as $\mathbf{r}_u = (r_u, \varphi_u)$, where

$$r_u = \Delta r(\varepsilon_u - 1/2),$$
$$\varphi_u = \frac{\pi\left[u - 4(\varepsilon_u - 1)^2 - 1/2\right]}{2(2\varepsilon_u - 1)}, \tag{14}$$

$u = 1, \ldots, W_1$, $\varepsilon_u = \sum_{n=0}^{N-1} \alpha_n(u)$ gives the number of ring on which the element is located, $\alpha_n(u) = 1$ when $u > 4n^2$ and $\alpha_n(u) = 0$ otherwise. The used surface discretization has been shown in Fig. 3. The angular size of the element depends on its number u and can be expressed as $(\Delta\varphi)_u = \pi/[2(2\varepsilon_u - 1)]$. Additionally, the set of vectors $\mathbf{r}'_q = (r_u, \varphi'_u)$, where

$$\varphi'_u = \varphi_u - (\Delta\varphi)_u/2 = \frac{\pi\left[u - 4(\varepsilon_u - 1)^2 - 1\right]}{2(2\varepsilon_u - 1)}, \tag{15}$$

has been used for the auxiliary discretization in the Rayleigh's method.

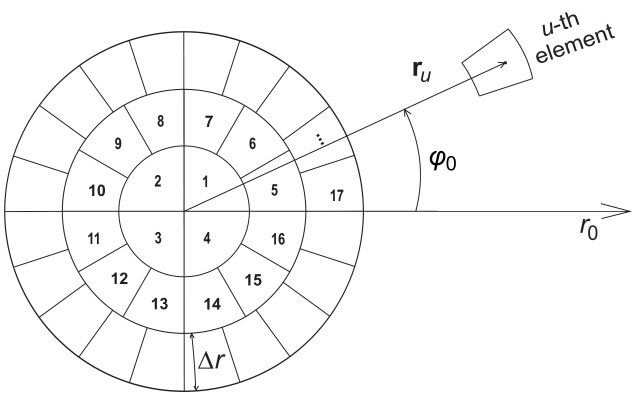

Fig. 3. The location of some elements for used surface discretization proposed by Arenas (2009a) (cf. his Sec. 2.3 and Fig. 1), the vector $\mathbf{r}_u$ defining the location of u-th element and the coordinates (r_0, φ_0) of the position vector $\mathbf{r}_0$.

8. Numerical analysis

The numerical calculations has been performed for the speed of sound equal to $c = 345.757$ m/s. It should be noted that the normalized sound power does not depend on the density of medium ρ_0. The sound radiation has been analyzed for the vibration frequencies $f \leq 1.1$ kHz, i.e., for $\lambda > 0.314$ m. It should be noted that some acoustic waves reflected from the floor generate the acoustic pressure which acts on the plate surface. This pressure value has been estimated in Apppendix A. It has been shown that the strongest influence of the waves reflected from the floor on the plate vibrations can be observed in the case when the vibration frequency is equal to $f = cn/(2l)$, where $n = 0, 1, \ldots$, and $l = 0.748$ m is the distance between the floor and the plate surface, which gives $f = 231.1$ Hz, 462.2 Hz, 693.4 Hz, and 924.5 Hz. Therefore, it can be expected that the measurement results obtained for the vibration frequencies close to these frequencies can not be accurate or even correct. The discretization with the elements' sizes smaller than $\lambda/6$ has to be used to obtain some correct results. It can be estimated that in this case, the relative error is less than about 15%. However, as smaller the elements' sizes as more accurate results. Since the analyzed object is the two coupled plates system, it is necessary to assume that the element sizes should also be much less than the shortest considered length of the plate bending wave. Taking into account that the vibration velocity amplitudes on the thin plate are considerably greater than the vibration velocity amplitudes on the baffle, it is enough to analyze the bending waves on the thin plate only. The length of the bending wave on the thin plate is given by (cf. Leissa (1969) Eq. (1.5); and Rao (2007) Eq. (14.225))

$$\lambda_p = \sqrt[4]{4\pi^2 D/(\rho h f^2)}, \tag{16}$$

where $D = Eh^3/[12(1-\nu^2)]$ is the plate's bending stiffness (cf. Leissa (1969) Eq. (1.2); and Rao (2007) Eq. (14.19)), E denotes the Young's modulus, ν is the Poisson's ratio and ρ is the plate's density. It has also been accepted that $E = 210$ GPa, $\nu = 0.3$, and $\rho = 7850$ kg/m^3 for the considered steel plate. It results in $\lambda_p > 0.1$ m and implies that the element sizes should be much less than 0.1 m. To satisfy this condition, the discretization of surface S_1 has been performed for $N = 75$ which means that the considered region has been divided into $W_1 = 4N^2 = 22\,500$ elements. It can be estimated that the element sizes are equal to $\Delta r = a_1/N = 6$ mm and $\Delta S/\Delta r = \pi a_1/(4N) \approx 5$ mm. Now, knowing that $\lambda_p/\Delta r > 16.7$, $\lambda_p \Delta r/\Delta S > 20$, $\lambda/\Delta r > 52$ and $\lambda\Delta r/\Delta S > 62$, the elements can be considered as small enough and the results of performed numerical analysis reliable.

8.1. Baffle's contribution to the sound radiation of the considered system

In order to determine the normalized sound power of the considered coupled plates system, it is necessary to taking into account the sound radiation by the surfaces of both plates. The large baffle's area causes that the vibration velocity measurements can be time-consuming. Moreover, the calculations of the sound

power with the use Hashimoto's method can also be time-consuming or even impossible to perform which is due to a large number of discretization elements. Therefore, in such case, another methodology for determining the sound power has to be proposed. Only thin circular plate is excited hence it can be expected that in some case, this plate gives a main contribution to the sound radiation of the considered system. This causes that the baffle's contribution can be neglected and the sound power of the considered system can approximately be determined based on measurements and calculations performed for the thin plate's surface only. This significantly reduces the number of points at which the vibration velocity has to be measured and makes the numerical calculations of the sound power possible to perform. It is of practical importance to indicate the conditions under which such simplification can be used. For this purpose, the baffle's contribution to the sound radiation of the considered system should be compared with the thin plate's contribution. However, comparing the sound power emitted by the baffle with the sound power radiated by the thin plate leads to time-consuming calculations. Therefore, it has been proposed that the contribution of vibrating surface to the sound radiation by the considered system can be estimated based on the time-average mean square vibration velocity. This quantity given by Eq. (4) is much easier to calculate than the sound power calculated from Eq. (5). In the case of the whole analyzed surface S_1, the formula for $\langle |v|^2 \rangle_{S_1}$ given by a single sum contains W_1 terms whereas the formula for Π expressed in the form of double sums contains $W_1(W_1+1)/2$ terms. Taking into account of numbers of terms in these formulas, it can be estimated that the calculations time of sound power is about $(W_1+1)/2 = 11\,250$ times longer than the calculations time of time-average mean square vibration velocity.

In order to indicate the cases for which the baffle's contribution can be neglected in the determining the normalized sound power of the considered coupled plates system, it is convenient to define the following quotient

$$q = \frac{\langle |v|^2 \rangle_{S_b}}{\langle |v|^2 \rangle_{S}}, \tag{17}$$

where S_b is the baffle's surface containing points for which $a < r_0 \leq a_1$. Making use of Eqs. (4) and (13), the above definition can be expressed as

$$q = \frac{S}{S_b} \frac{\sum\limits_{u=W+1}^{W_1} |\beta_u|^2}{\sum\limits_{u=1}^{W} |\beta_u|^2}, \tag{18}$$

where $\beta_u = \beta(\mathbf{r}_u)$. The quantity q depends only on the values of the coefficient $\beta(\mathbf{r}_0)$ and depends neither on the excitation force F nor on the vibration velocity v. To show the thin plate's vibration response as well as the baffle's contribution to the sound power of the considered system, the normalized quantity $\langle |v|^2 \rangle_S / F^2$ [m^2/(s^2·N^2)] calculated with the use of Eqs. (4) and (13) and the quotient q have been presented in Fig. (4) as a function of the vibration frequency.

It has been assumed that for $q < 0.01$, the baffle's contribution to the sound power of the considered system is negligible small and the proposed methodology to approximately determine the sound power of the analyzed coupled plates as the sound power radiated only by the thin plate can be employed. Figure 4 proves that these cases occur for the wide frequency ranges, for example, $f \in (100, 200)$ Hz, $f \in (350, 550)$ Hz as well as $f \in (850, 1100)$ Hz. Some small values of q have been observed both for the vibration frequencies close to the resonances frequencies and for some other ones. For example, in Fig. 4b, the analyzed quantities has been presented additionally for the narrow frequency range related to one of the resonance frequencies. Based on Fig. 4b, it can be concluded that for the vibration frequencies close to the resonance frequency equal to about 103 Hz, the thin plate gives a main contribution to the sound power of the considered system and the proposed methodology can be used. In the case of low frequencies, i.e., when $f < 80$ Hz, the quotient q assumes some greater values, $q > 0.1$ which shows a significant baffle's contribution to the sound radiation of the considered system. Thus, it can be stated that the

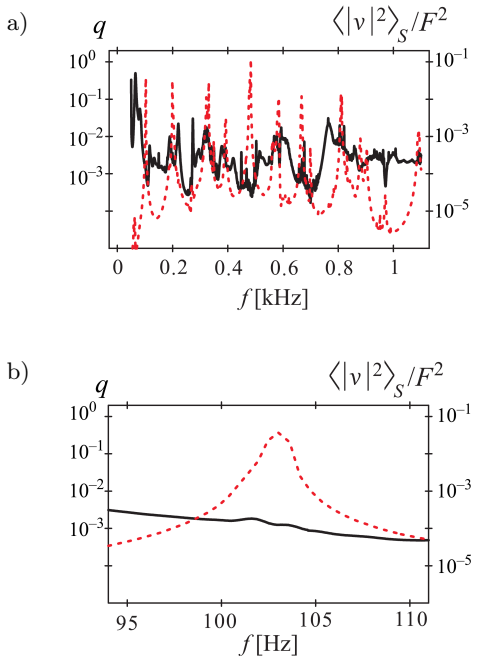

Fig. 4. The quotient q given by Eq. (17) – solid line and the normalized time-average mean square vibration velocity $\langle |v|^2 \rangle_S / F^2$ – dashed line as the functions of vibration frequency: a) whole analyzed frequency range, b) narrow frequency range around the resonance frequency of the considered system.

normalized sound power at low frequencies has to be determined by taking into account the sound radiation by surfaces of both plates.

8.2. Normalized sound power

Inserting Eq. (13) into Eqs. (4) and Eq. (5) or alternatively (11), the normalized sound power $\Pi/\Pi^{(\infty)}$ can be expressed by means of the proportional coefficient $\beta(\mathbf{r}_0)$. Because of the high computational complexity of the analyzed problem, the numerical analysis has been performed taking into account the thin plate's surface only. Therefore, the obtained results are valid for the considered coupled plates system only in the case when the baffle's contribution is small enough to be neglected, i.e., when the quotient $q < 0.01$. On the basis of the measurement data and using the Hashimoto's method, the radiation efficiency σ and the added mass coefficient κ have been calculated and presented in Fig. 5 as the functions of the vibration frequency. The imaginary part of self impedance $Z^{(\mathrm{self})}$ from Eq. (6) is given by the Struve function of first order $\mathbf{H}_1(x)$. The numerical estimation of the value for this function can be time consuming. Therefore, the following approximation proposed by Aarts and Janssen (2003) (cf. their Eq. (16))

$$\mathbf{H}_1(x) \simeq \frac{2}{\pi} - J_0(x) + \left(\frac{16}{\pi} - 5\right)\frac{\sin x}{x} + \left(12 - \frac{36}{\pi}\right)\frac{1-\cos x}{x^2}, \tag{19}$$

has been used to improve the numerical calculations. In order to check the validity of the proposed Rayleigh's method, for comparison, the quantities σ and κ have also been calculated from the formula given by Eq. (11). Assuming that the results given by the Hashimoto's method are exact, the percentage relative error has been estimated for the results obtained on the basis of the Rayleigh's method. The relative error for σ does not exceed 3%. The only exceptions are very narrow frequency ranges for which it is greater than 3% and does not exceed 12.2%. In the case of the added mass coefficient κ, it has been estimated that the relative error is less than 1% with the exception of a very narrow frequency range for which it exceeds 1% but is less than 4%. Taking into account the value of the relative error, it can be stated that both methodologies lead to equivalent results. Taking into account that the number of terms in Eq. (11) is about two times greater than the number of terms in the formula from Eq. (5), it is obvious that the Hashimoto's method has a greater computational efficiency than the Rayleigh's method. However, the advantage of the formula given by Eq. (11) is the fact that it is not expressed by the special functions such as the Bessel or Struve functions which makes it easier for further implementations.

It is of interest to compare the experimental results obtained for the thin plate with the results given by a pure theoretical model. It gives the answer whether the Hashimoto's method is correct. The measurements of the vibration velocity shown that the thin plate's vibrations are transmitted to the baffle by its edge. Hence, the analyzed thin plate can not be considered as the perfectly clamped circular plate. In order to theoretically predict its behavior, its boundary conditions have to be describe with the use of more complicated model. In the literature, the elastically supported edge, whose properties are defined by two stiffness constants, has been proposed to describe the real boundary conditions. The sound power of the circular plate for such boundary conditions has been discussed by Rdzanek *et al.* (2003; 2007) in the case of the point excitation and when the internal as well as acoustic damping are neglected. It is of interest to examine whether this theoretical model is accurate enough to predict the sound radiation of analyzed plate. For this purpose, it is necessary to find the values of dimensionless stiffness constants $\overline{K}_W = K_W a^3/D$ and $\overline{K}_\psi = K_\psi a/D$, where K_W and K_ψ are the boundary stiffness constant associated with the force counteracting the transverse deflection of the plate's edge and the rotary moment, respectively. The normalized sound power has been calculated for some different values of $\overline{K}_W$ and $\overline{K}_\psi$. Finally, it has been assumed that $\overline{K}_W = 1200$ and $\overline{K}_\psi = 1000$ which allows the results obtained with the use of the theoretical model to be as close as possible to those obtained based on the measurements. In Fig. 5, for comparison, the curves given by the theoretical formulas have been presented together with the curves obtained based on the measurement data. In the case of σ, a good agreement between those curves is observed for the vibration frequency $f < 0.6$ kHz with the exception of some very narrow frequency ranges. At higher frequencies, the results obtained with the use of both methodology can significantly differ from each other. This effect can be explained by the fact that the increase in frequency leads to the increase in the size

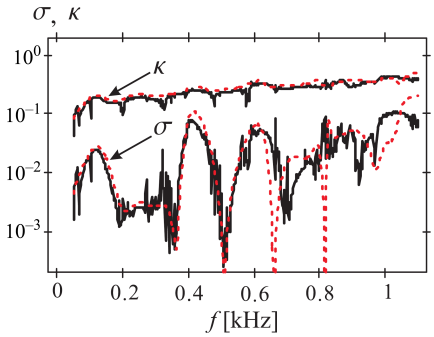

Fig. 5. The radiation efficiency σ and the added mass coefficient κ as the functions of the vibration frequency. The line keys: solid – obtained on the basis of measurement data with the use of the Hashimoto's method, dashed – obtained from the theoretical model.

of discretization elements compared with the length of acoustic wave λ. For the added mass coefficient κ, Fig. 5 shows a good agreement between experimental and theoretical curve for the whole analyzed frequency range.

9. Conclusions

The normalized sound power of the two coupled plates system of practical importance has been analyzed. The considered object was the thin circular plate with a point excitation which has been mounted to the thick flat baffle. The results of the performed investigations and analysis can be summarized as follows:

1) Taking into account that experimental investigations of the sound power are difficult or in some cases even impossible, the useful methodology has been proposed. This approach is based on the observation that in some cases the baffle's contribution to the sound radiation can be neglected. The criterion indicating these cases has been defined.
2) Based on the simple theoretical model, the frequencies, for which the strongest influence of acoustic waves reflected from the floor can occur, have been indicated.
3) The equivalent formula for the Hashimoto's method has been presented without the use of the special function such as the Bessel and the Struve function. Its advantage is a simpler implementation in a programming language.
4) For comparison, the theoretical model of elastically supported plate has been used to determine the normalized sound power of the thin circular plate which is the part of considered system. A good agreement between theoretical and experimental results has been obtained in the case when the vibration frequency is less than 0.6 kHz. This proves that at low frequencies, the behavior of a real circular plate can be predicted based on the pure theoretical formulas. Moreover, it can be concluded that the Hashimoto's method gives some accurate results only for the frequencies less than 0.6 kHz.

Appendix

Eigenvalues of the fluid layer

The problem of the resonance frequencies of the fluid layer can be considered roughly as a single dimensional problem. The simplifying assumption is that the entire plane is vibrating with a uniform normal velocity. The flat wave conditions can be actually satisfied in the rigid tube below the first non-zero eigenvalue (cf. Beranek (1996) Eq. (2.47), p. 32 for the rigid termination; and Beranek and Mellow (2012) Eq. (2.58), p. 38 for the impedance termination). The acoustic pressure satisfies the following single dimensional Helmholtz equation in the fluid layer

$$\frac{\mathrm{d}^2 p}{\mathrm{d}z^2} + k^2 p = 0, \tag{20}$$

for $0 \geqslant z \geqslant -l$, and $p(z,t) = p(z)\exp(-\mathrm{i}\omega t)$.

Generally, the impedance boundary condition can be derived from the law of conservation of momentum (cf. Kuttruff (2009) Eq. (1.2) p. 8)

$$\nabla p + \varrho_0 \frac{\partial \mathbf{v}}{\partial t} = 0, \tag{21}$$

and from the wall impedance definition (cf. Kuttruff (2009) Eq. (2.2), p. 37, and Kuttruff (2007) Sec. 7.1)

$$Z = \left(\frac{p}{v_n}\right)_{\text{surface}}, \tag{22}$$

where $v_n = \mathbf{n}\cdot\mathbf{v}$, $\mathbf{n}$ is the unit vector outward normal to the boundary surface. Now, multiplying Eq. (21) side by side by $\mathbf{n}$ and differentiating Eq. (22) with respect to time t, gives finally, the impedance boundary condition in the following form (cf. Kuttruff (2009) Eqs. (3.2a) and (3.2b), p. 68; Meissner (2013) Eq. (2); Meissner (2015) Eq. (5))

$$\begin{aligned} \frac{\partial p}{\partial n} + \frac{\beta}{c}\frac{\partial p}{\partial t} &= 0, \\ \frac{\partial p}{\partial n} - \mathrm{i}k\beta p &= 0, \end{aligned} \tag{23}$$

where $\partial p/\partial n = \mathbf{n}\cdot\nabla p$, $\mathbf{n}$ is the unit vector outward normal to the boundary surface, $\beta = \varrho_0 c/Z$ is the dimensionless floor admittance, and c is the sound velocity in fluid.

The following boundary conditions are satisfied

$$\begin{aligned} \left.\frac{\mathrm{d}p}{\mathrm{d}z}\right|_{z=-l} &= -\mathrm{i}k\beta p(-l), \\ \left.\frac{\mathrm{d}p}{\mathrm{d}z}\right|_{z=0} &= +\mathrm{i}k\varrho_0 c v_0, \end{aligned} \tag{24}$$

where v_0 is the normal outward vibration velocity on the upper plane bounding the fluid layer.

The solution to Eq. (20) may be expected in the general form of

$$p(z) = A(k)\sin[k(z+l/2)] + B(k)\cos[k(z+l/2)]. \tag{25}$$

Inserting this solution to the boundary conditions yields immediately

$$\begin{aligned} &A(k)\Big[\cos(kl/2) - \mathrm{i}\beta\sin(kl/2)\Big] \\ &\quad + B(k)\Big[\sin(kl/2) + \mathrm{i}\beta\cos(kl/2)\Big] = 0, \\ &A(k)\cos(kl/2) - B(k)\sin(kl/2) = +\mathrm{i}\varrho_0 c v_0. \end{aligned} \tag{26}$$

These two equations can be solved with respect to $A(k)$ and $B(k)$, giving

$$A(k) = +\mathrm{i}\varrho_0 c v_0 \frac{\sin(kl/2) + \mathrm{i}\beta\cos(kl/2)}{\sin(kl) + \mathrm{i}\beta\cos(kl)};$$
$$\lim_{\beta\to 0} A(k) = \frac{+\mathrm{i}\varrho_0 c v_0}{2\cos(kl/2)},$$
$$B(k) = -\mathrm{i}\varrho_0 c v_0 \frac{\cos(kl/2) - \mathrm{i}\beta\sin(kl/2)}{\sin(kl) + \mathrm{i}\beta\cos(kl)};$$
$$\lim_{\beta\to 0} B(k) = \frac{-\mathrm{i}\varrho_0 c v_0}{2\sin(kl/2)}. \tag{27}$$

Inserting these back into Eq. (25) provides the acoustic pressure in the form of

$$p(z) = \frac{\mathrm{i}\varrho_0 c v_0}{\sin(kl) + \mathrm{i}\beta\cos(kl)} \cdot \Big\{ [\sin(kl/2) + \mathrm{i}\beta\cos(kl/2)]\sin[k(z+l/2)] - [\cos(kl/2) - \mathrm{i}\beta\sin(kl/2)]\cos[k(z+l/2)] \Big\},$$
$$\lim_{\beta\to 0} p(z) = \frac{1}{2}\mathrm{i}\varrho_0 c v_0 \left[\frac{\sin[k(z+l/2)]}{\cos(kl)} - \frac{\cos[k(z+l/2)]}{\sin(kl/2)} \right]. \tag{28}$$

Then, the following functions can be obtained at both fluid bounding planes

$$p(-l) = \frac{-\mathrm{i}\varrho_0 c v_0}{\sin(kl) + \mathrm{i}\beta\cos(kl)};$$
$$\lim_{\beta\to 0} p(-l) = -\frac{\mathrm{i}\varrho_0 c v_0}{\sin(kl)},$$
$$p(0) = -\mathrm{i}\varrho_0 c v_0 \frac{\cos(kl) - \mathrm{i}\beta\sin(kl)}{\sin(kl) + \mathrm{i}\beta\cos(kl)};$$
$$\lim_{\beta\to 0} p(0) = -\mathrm{i}\varrho_0 c v_0 \frac{\cos(kl)}{\sin(kl)}. \tag{29}$$

The eigenvalues are complex when $\beta \neq 0$, whereas when $\beta = 0$, the characteristic equation is

$$\sin(kl) = 0; \qquad k = n\frac{\pi}{l}; \qquad n = 0, 1, 2, \ldots, \tag{30}$$

i.e. the acoustic pressure maximums occur on both planes (the upper and the lower, no matter which plane is the driving plane) whenever this equation is satisfied. On the other hand the acoustic pressure nodes occur only on the upper plane (on the lower plane a minimum occurs) whenever

$$\cos(kl) = 0; \quad k = \left(m + \frac{1}{2}\right)\frac{\pi}{l}; \quad m = 0, 1, 2, \ldots \tag{31}$$

Acknowledgments

The research presented in this paper was partially supported under The Centre for Innovation and Transfer of Natural Sciences and Engineering Knowledge Project at The University of Rzeszów in Poland.

References

1. Aarts R.M., Janssen A.J.E.M. (2003), *Approximation of the Struve function H1 occurring in impedance calculations*, Journal of the Acoustical Society of America, **113**, 5, 2635–2637, doi: 10.1121/1.1564019.
2. *Amabili M., Frosali G., Kwak M.K.* (1996), *Free vibrations of annular plates coupled with fluids*, Journal of Sound and Vibration, **191**, 5, 825–846, doi: 10.1006/jsvi.1996.0158.
3. Arenas J.P. (2008), *Numerical computation of the sound radiation from a planar baffled vibrating surface*, Journal of Computational Acoustics, **16**, 3, 321–341, doi: 10.1142/S0218396X08003671.
4. Arenas J.P. (2009a), *On the sound radiation from a circular hatchway*, International Journal of Occupational Safety and Ergonomics, **15**, 4, 401–407, doi: 10.1080/10803548.2009.11076819.
5. Arenas J.P. (2009b), *Matrix method for estimating the sound power radiated from a vibrating plate for noise control engineering applications*, Latin American Applied Research, **39**, 4, 345–352.
6. Arenas J.P. (2010), *Calculation of the energy of elastically supported isotropic circular plates at flexural modal vibration frequencies*, 17th International Congress on Sound and Vibration 2010, ICSV 2010, **2**, 1536–1543.
7. Arenas J.P., Crocker M.J. (2002), *Sound radiation efficiency of a baffled rectangular plate excited by harmonic point forces using its surface resistance matrix*, International J. Acoustics and Vibration, **7**, 4, 217–229.
8. Beigelbeck R., Antlinger H., Cerimovic S., Clara S., Keplinger F., Jakoby B. (2013), *Resonant pressure wave setup for simultaneous sensing of longitudinal viscosity and sound velocity of liquids*, Measurement Science and Technology, **24**, 12, 125101, doi: 10.1088/0957-0233/24/12/125101.
9. Beranek L.L. (1996), *Acoustics*, Acoustical Society of America, New York.
10. Beranek L.L., Mellow T.J. (2012), *Acoustics: sound fields and transducers*, Academic Press, New York.
11. Brański A., Szela S. (2011), *Evaluation of the active plate vibration reduction by the parameter of the acoustic field*, Acta Physica Polonica A, **119**, 6A, 942–945.
12. Chiang H.-Y., Huang Y.-H. (2015), *Vibration and sound radiation of an electrostatic speaker based on circular diaphragm*, Journal of the Acoustical Society of America, **137**, 4, 1714–1721, doi: 10.1121/1.4916275.
13. Chiang H.-Y., Huang Y.-H. (2018), *Resonance mode and sound pressure produced by circular diaphragms of electrostatic and piezoelectric speakers*, Applied Acoustics, **129**, 365–378, doi: 10.1016/j.apacoust.2017.08.020.

14. Christiansen T.L., Hansen O., Thomsen E.V., Jensen J.A. (2014), *Modal radiation patterns of baffled circular plates and membranes*, Journal of the Acoustical Society of America, **135**, 5, 2523–2533, doi: 10.1121/1.4869688.
15. Díaz-Cereceda C., Poblet-Puig J., Rodríguez-Ferran A. (2012), *The finite layer method for modelling the sound transmission through double walls*, Journal of Sound and Vibration, **331**, 22, 4884–4900, doi: https://doi.org/10.1016/j.jsv.2012.06.001.
16. Gazizullin R.K., Paimushin V.N. (2016), *The transmission of an acoustic wave through a rectangular plate between barriers*, Journal of Applied Mathematics and Mechanics, **80**, 5, 421–432, doi: 10.1016/j.jappmathmech.2017.02.009.
17. Hasheminejad S., Afsharmanesh B. (2014), *Vibroacoustic response of an annular sandwich electrorheological disc*, Journal of Low Frequency Noise Vibration and Active Control, **33**, 3, 371–394, doi: 10.1260/0263-0923.33.3.371.
18. Hasheminejad S.M., Keshavarzpour H. (2016), *Robust active sound radiation control of a piezo-laminated composite circular plate of arbitrary thickness based on the exact 3d elasticity model*, Journal of Low Frequency Noise Vibration and Active Control, **35**, 2, 101–127, doi: 10.1177/0263092316644085.
19. Hashimoto N. (2001), *Measurement of sound radiation efficiency by the discrete calculation methods*, Applied Acoustics, **62**, 429–446, doi: 10.1016/S0003-682X(00)00025-6.
20. Hu H.H., Shang D.J. (2012), *A fast method for the sound radiation of baffled rectangular plate with fluid loading*, In 2012 IEEE International Conference on Mechatronics and Automation, pp. 1318–1322, doi: 10.1109/ICMA.2012.6284327.
21. Jeong K.-H. (2003), *Free vibration of two identical circular plates coupled with bounded fluid*, Journal of Sound and Vibration, **260**, 4, 653–670, doi: 10.1016/S0022-460X(02)01012-X.
22. Jeong K.-H., Kim K.-J. (2005), *Hydroelastic vibration of a circular plate submerged in a bounded compressible fluid*, Journal of Sound and Vibration, **283**, 1-2, 153–172, doi: 10.1016/j.jsv.2004.04.029.
23. Jiang C.H., Kam T.Y., Chang Y.H. (2017), *Sound radiation of panel-form loudspeaker using flat voice coil for excitation*, Applied Acoustics, **116**, 375–389, doi: 10.1016/j.apacoust.2016.10.009.
24. Jung J., Kook J., Goo S., Wang S. (2017), *Sound transmission analysis of plate structures using the finite element method and elementary radiator approach with radiator error index*, Advances in Engineering Software, **112**, 1–15, doi: 10.1016/j.advengsoft.2017.06.001.
25. Kamper M., Bekker A. (2017), *Non-contact experimental methods to characterise the response of a hyper-elastic membrane*, International Journal of Mechanical and Materials Engineering, **12**, 1, 1–16, doi: 10.1186/s40712-017-0082-6.
26. Kolber K., Snakowska A., Kozupa M. (2014), *The effect of plate discretization on accuracy of the sound radiation efficiency measurements*, Archives of Acoustics, **39**, 4, 511–518, doi: 10.2478/aoa-2014-0055.
27. Kozupa M.M., Wiciak J.W. (2011), *Comparison of passive and active methods for minimization of sound radiation by vibrating clamped plate*, Acta Physica Polonica A, **119**, 6 A, 1013–1017.
28. Kuttruff H. (2007), *Acoustics. An Introduction*, Taylor and Francis, New York.
29. Kuttruff H. (2009), *Room Acoustics*, Taylor and Francis, New York.
30. Kwak M.K., Kim K.C. (1991), *Axisymmetric vibration of circular plates in contact with fluid*, Journal of Sound and Vibration, **146**, 3, 381–389, doi: 10.1016/0022-460X(91)90696-H.
31. Langfeldt F., Gleine W., von Estorff O. (2018), *An efficient analytical model for baffled, multi-celled membrane-type acoustic metamaterial panels*, Journal of Sound and Vibration, **417**, 359–375, doi: 10.1016/j.jsv.2017.12.018.
32. Lee M.-R., Singh R. (1994), *Analytical formulations for annular disk sound radiation using structural modes*, Journal of the Acoustical Society of America, **95**, 6, 3311–3323, doi: 10.1121/1.409993.
33. Leissa A.W. (1969), *Vibration of Plates*, Vol. SP-160 of NASA Technical Reports, National Aeronautics and Space Administration, Washington D.C., http://ntrs.nasa.gov/search.jsp?R=19700009156.
34. Leniowska L. (2006), *Effect of active vibration control of a circular plate on sound radiation*, Archives of Acoustics, **31**, 1, 77–87.
35. Leniowska L., Mazan D. (2015), *MFC sensors and actuators in active vibration control of the circular plate*, Archives of Acoustics, **40**, 2, 257–265, doi: 10.1515/aoa-2015-0028.
36. Liu R., Hao Z., Zheng X., Xiong F., Yang W., Jiang J. (2017), *The partially-coupled modal contribution assumption of noise radiation and the dominant noise-contribution mode*, Journal of Sound and Vibration, **389**, 266–275, doi: https://doi.org/10.1016/j.jsv.2016.10.046.
37. Luo Z., Hao Z.-Y., Zheng X. (2015), *Precision improvement of the discrete calculation method for sound radiation research*, Journal of Shanghai Jiaotong University (Science), **20**, 4, 415–419, doi: 10.1007/s12204-015-1616-9.
38. Matthews D., Sun H., Saltmarsh K., Wilkes D., Munyard A., Pan J. (2014), *A detailed experimental modal analysis of a clamped circular plate*, In Iner-Noise 2014, pp. 1–9, Melbourne, Australia, 16–19 November 2014.
39. Mazur K., Pawełczyk M. (2011), *Active noise-vibration control using the filtered-reference lms algorithm with compensation of vibrating plate temperature variation*, Archives of Acoustics, **36**, 1, 65–76, doi: 10.2478/v10168-011-0006-z.

40. Mazur K., Pawełczyk M. (2016), *Internal model control for a light-weight active noise-reducing casing*, Archives of Acoustics, **41**, 2, 315–322, doi: 10.1515/aoa-2016-0032.
41. Meissner M. (2013), *Acoustic behaviour of lightly damped rooms*, Acta Acustica united with Acustica, **99**, 5, 845–847, doi: 10.3813/AAA.918663.
42. Meissner M. (2015), *Prediction of reverberant properties of enclosures via a method employing a modal representation of the room impulse response*, Archives of Acoustics, **41**, 1, doi: 10.1515/aoa-2016-0003.
43. Oberst S., Lai J.C.S., Marburg S. (2013), *Guidelines for numerical vibration and acoustic analysis of disc brake squeal using simple models of brake systems*, Journal of Sound and Vibration, **332**, 9, 2284–2299, doi: 10.1016/j.jsv.2012.11.034.
44. Pritchard R.L. (1960), *Mutual acoustic impedance between radiators in an infinite rigid plane*, Journal of the Acoustical Society of America, **32**, 6, 730–737, doi: 10.1121/1.1908199.
45. Rao S.S. (2007), *Vibrations of continuous systems*, Wiley, New Jersey.
46. Rayleigh J.W.S. (1896), *The theory of sound*, Vol. 2, Macmillan, New York, 2nd ed.
47. Rdzanek W.P., Engel Z., Rdzanek W.J. (2003), *Theoretical analysis of sound radiation of an elastically supported circular plate*, Journal of Sound and Vibration, **265**, 1, 155–174, doi: 10.1016/S0022-460X(02)01445-1.
48. Rdzanek W.P., Rdzanek W.J., Engel Z., Szemela K. (2007), *The modal low frequency noise of an elastically supported circular plate*, International Journal of Occupational Safety and Ergonomics, **13**, 2, 147–157, doi: 10.1080/10803548.2007.11076718.
49. Rdzanek W.P., Rdzanek W.J., Szemela K. (2016), *Sound radiation of the resonator in the form of a vibrating circular plate embedded in the outlet of the circular cylindrical cavity*, Journal of Computational Acoustics, **24**, 4, 1650018, 23 pages, doi: 10.1142/S0218396X16500181.
50. Robin O., Chazot J.-D., Boulandet R., Michau M., Berry A., Atalla N. (2016), *A plane and thin panel with representative simply supported boundary conditions for laboratory vibroacoustic tests*, Acta Acustica united with Acustica, **102**, 1, 170–182, doi: 10.3813/AAA.918934.
51. Shahraeeni M., Shakeri R., Hasheminejad S.M. (2015), *An analytical solution for free and forced vibration of a piezoelectric laminated plate coupled with an acoustic enclosure*, Computers and Mathematics with Applications, **69**, 11, 1329–1341, doi: 10.1016/j.camwa.2015.03.022.
52. Skudrzyk E. (1971), *The Foundations of Acoustics*, Basic Mathematics and Basic Acoustics, Springer, New York.
53. Squicciarini G., Putra A., Thompson D.J., Zhang X., Salim M.A. (2015), *Use of a reciprocity technique to measure the radiation efficiency of a vibrating structure*, Applied Acoustics, **89**, 107–121, doi: 10.1016/j.apacoust.2014.09.013.
54. Sun Y., Pan J., Yang T. (2015), *Effect of a fluid layer on the sound radiation of a plate and its active control*, Journal of Sound and Vibration, **357**, 269–284, doi: https://doi.org/10.1016/j.jsv.2015.07.016.
55. Vishwakarma S.D., Pandey A.K., Parpia J.M., Southworth D.R., Craighead H.G., Pratap R. (2014), *Evaluation of mode dependent fluid damping in a high frequency drumhead microresonator*, Journal of Microelectromechanical Systems, **23**, 2, 334–346, doi: 10.1109/JMEMS.2013.2273803.
56. Wang X., Xiang Y. (2017), *Probes design and experimental measurement of acoustic radiation resistance*, International Journal of Acoustics and Vibrations, **22**, 2, 252–259, doi: 10.20855/ijav.2017.22.2471.
57. Wiciak J. (2007), *Modelling of vibration and noise control of a submerged circular plate*, Archives of Acoustics, **32**, 4S, 265–270, http://acoustics.ippt.pan.pl/index.php/aa/article/view/1419/1236.
58. Xiaoqing W., Yang X., Zhiyong G., Xuebao X., Yuxiao S., Peng X., Shaowei W. (2014), *Research on experimental measurement of acoustic resistance and major accuracy influencing factors analysis*, Journal of Mechanical Science and Technology, **28**, 4, 1219–1227, doi: 10.1007/s12206-014-0302-1.
59. Yuan M., Qiu J., Ji H. (2011), *Stiffened panel sound radiation attenuation using acceleration feedback and internal model control*, In 2011 Symposium on Piezoelectricity, Acoustic Waves and Device Applications (SPAWDA), pp. 554–557, doi: 10.1109/SPAWDA.2011.6167311.
60. Yuan M., Ji H., Qiu J., Ma T. (2012), *Active control of sound transmission through a stiffened panel using a hybrid control strategy*, Journal of Intelligent Material Systems and Structures, **23**, 7, 791–803, doi: 10.1177/1045389X12439638.
61. Zhao J., Qiu J., Ji H. (2016), *Reconstruction of the nine stiffness coefficients of composites using a laser generation based imaging method*, Composites Science and Technology, **126**, 27–34, doi: 10.1016/j.compscitech.2016.02.001.